Visual Through Infrared: Modeling Components and Methodologies for Estimating High Fidelity Ground Vehicle Signatures

William R. Reynolds
Signature Research, Inc.
P.O. Box 346
Calumet, Michigan 49913
USA
reynolds@signatureresearchinc.com

Abstract

For a number of reasons there has been increased recognition that physics based signature models are crucial to the defense industry. Consequently, several new modeling initiatives have been started and current tools continue to be maintained and supported. For example, deficiencies in ground vehicle exhaust plume signatures and high spatial and radiometric fidelity background signatures are currently being remedied. In addition, increased emphasis is being given to capturing detailed target and background interactions.

The methodologies for obtaining both visual and IR state-of-the-art ground vehicle signatures will be reviewed. In addition, a next generation physics based modeling effort will be introduced which involves massive integration of current models. Results will be presented and future efforts will be discussed.

1 Introduction

The first clear articulation of a physics-based ground vehicle model was a final report which was the result of a year and a half study for the Rome Air Development Center at Griffis Air Force Base by the University of Michigan's Infrared and Optics Laboratory of Willow Run Laboratories (currently a division of General Dynamics) in Ann Arbor, Michigan [1]. The contract started in December of 1967 and was completed in June of 1969. Most noteworthy was, "*A computerized mathematical model for the prediction of time-dependent surface temperatures and radiances of planar targets and backgrounds has been formulated.*" And furthermore, "*Additional capabilities of the model include estimates of target-background contrast as a function of time-dependent meteorological environments and scanner parameters...*" In conclusion, "*The validity of the model has been established directly by experimental measurements and indirectly through the use of infrared imagery.*" In one stroke, facetized geometry, dynamic target and background models, and validation are covered in detail.

From this early Willow Run Laboratories effort to present day there has been steady pressure for signature model technology development in terms of photo-realism with a physics-based constraint. Figure 1 is a notional graph detailing the modeling development timeline and also illustrating the progression in complexity. Models that were somewhat widely known and ones that represent a new capability were given an arbitrary complexity rating which then plotted versus their nominal release dates. Complexity is an ad hoc rating of algorithmic and computation sophistication coupled with spatial fidelity.

The Willow Run report [1] and others [2, 3, 4] prove that signature modeling complexity has only been limited by the computing resources. The algorithms and approach contained within the report are every bit as detailed as the current MuSES and CAMEOSIM. Currently the standard is 100s of millions of polygons as found in the CAMEOSIM and *EOView* applications.

Paper presented at the RTO SCI Symposium on "Sensors and Sensor Denial by Camouflage, Concealment and Deception", held in Brussels, Belgium, 19-20 April 2004, and published in RTO-MP-SCI-145.

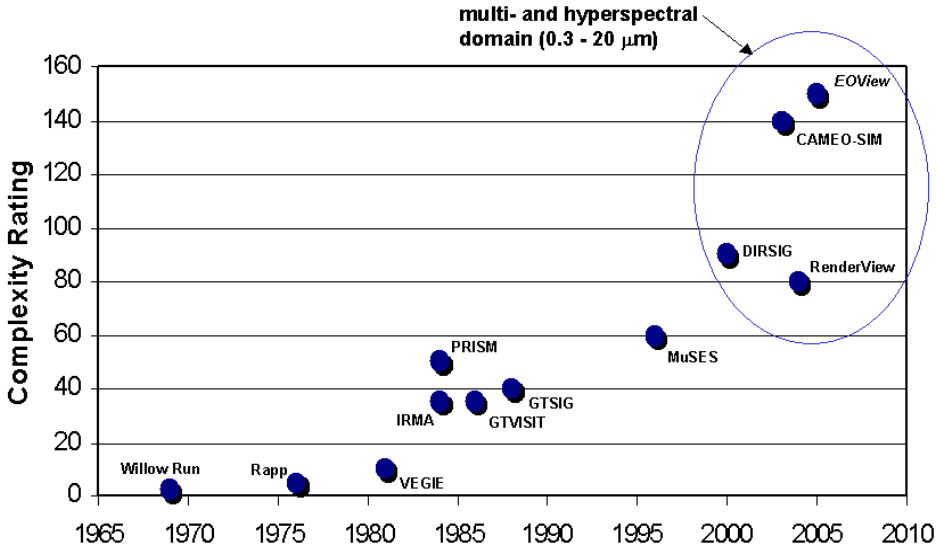

Figure 1: Notional complexity of signature modeling development plotted against approximate public release.

The *EOView* model is being designed to run on modern computing clusters and high performance multi-processor computing resources. For example, a 16 node Beowulf cluster, with gigahertz plus processors can reach 180 gflops of peak computational speed for the cost of a low end Silicon Graphics workstation in the early nineties, about 30,000 dollars. Photo-realistic target and background models are now unequivocally feasible.

It is somewhat clear that the remaining decade will be spent fleshing out details in large scale scene modeling by incorporating 3-dimensional target and background interaction, exhaust plumes, articulation, and target translation. In addition, battlefield effects including dust, smoke, and gun flash will become standard in the next generation models. Multiple vehicles in scenes in the best Lucas film tradition will be standard with one critical difference...the target and scene phenomenology are physics-based.

If the signature phenomenology can be captured in the models and the output is photo-realistic then camouflage design and integration can be taken into the laboratory where the process becomes immensely less expensive. The rendered output images can be incorporated into a perception laboratory which allow the signatures to be efficiently evaluated by human observers. One observer can evaluate approximately 400 images in a half of a day. 30 to 60 subjects can completely quantify 10 or more camouflage alternatives in a weeks time. The camouflage performance can be quantified in terms of the probabilities of acquisition as a function of range or search time. Contrast the laboratory approach with the complexity of a full scale field exercise involving 60 observers and as many support staff over a 6 or 8 week period of time to achieve comparable statistical significance.

2 *RenderView*

One can consider *RenderView*, a Signature Research tool developed with TARDEC sponsorship, to be a intermediate step in the progression from high fidelity target models to integrated target and background predictive models. The resultant rating is shown in figure 1. *RenderView* uses a measured, spatially differentiated background, to provide the input radiation field at the target. The target is then rendered using ray tracing and the bidirectional reflectance distribution function (BRDF) of the target surface. The rendered target is then inserted into the corresponding "at range" image to create a phenomenologically correct photo-realistic image. Figure 2 is an example of this process in the visible band.

Figure 3 is a block diagram showing the phenomenology, inputs, and outputs of the *RenderView* approach.

Figure 2: A MBT rendered in *RenderView* and inserted into a measured background.

The inputs include the object geometry, the panoramic radiation field, and other meteorological and geographic data that is required. Most importantly, *RenderView* incorporates the BRDF in the rendering process. Consequently, energy for each pixel is the weighted sum of the reflections from the surrounding hemisphere of spatially differentiated pixels of the calibrated panoramic image.

2.1 Panoramic Data Collection System

RenderView operates in both the reflective and reflective/emissive spectral domains. Consequently, the background and target reflectivity data must be consistent and both determine the rendered output. Therefore, the primary data required for *RenderView* is the calibrated panoramic and "at range" images. The advantage is that just the data acquisition equipment needs to be taken to the field and not the actual test articles.

A methodology for collecting the background data in the visual (RGB) domain has been developed. Special purpose hardware and software has been created to efficiently collect the calibrated visual band background data sets. A diagram of the calibrated background acquisition system is shown in figure 4. The Nikon model D100 cameras are currently being used to collect the panoramic images. A Nikon D1x is used to collect the "at range" data. All of the images are collect in the .nef format. This format is unprocessed focal plane data and requires significant post processing. Calibration is achieved by an absolute calibration of the Nikon cameras using a Hoffman source. This is backed up by placing a Macbeth ColorChecker set of standards in each image.

Using telemetry to trigger the shutters we estimate that the three shutters are triggered within 35 msec. This simultaneity is required because of the rapid imperceptible fluctuations in illumination.

To date some LWIR scene data has been also acquired by painstaking means. The panoramas have been acquired by rotating the imager on a tripod. Typically two passes are required for a nearly complete data set. The successive images are then adjusted and stitched together. Missing zenith sky data is estimated and filled in. Discussions are underway to develop a panoramic system using parabolic front surface mirrors similar to the RGB system. In general, the spatial resolution of the panoramic images is not stringent.

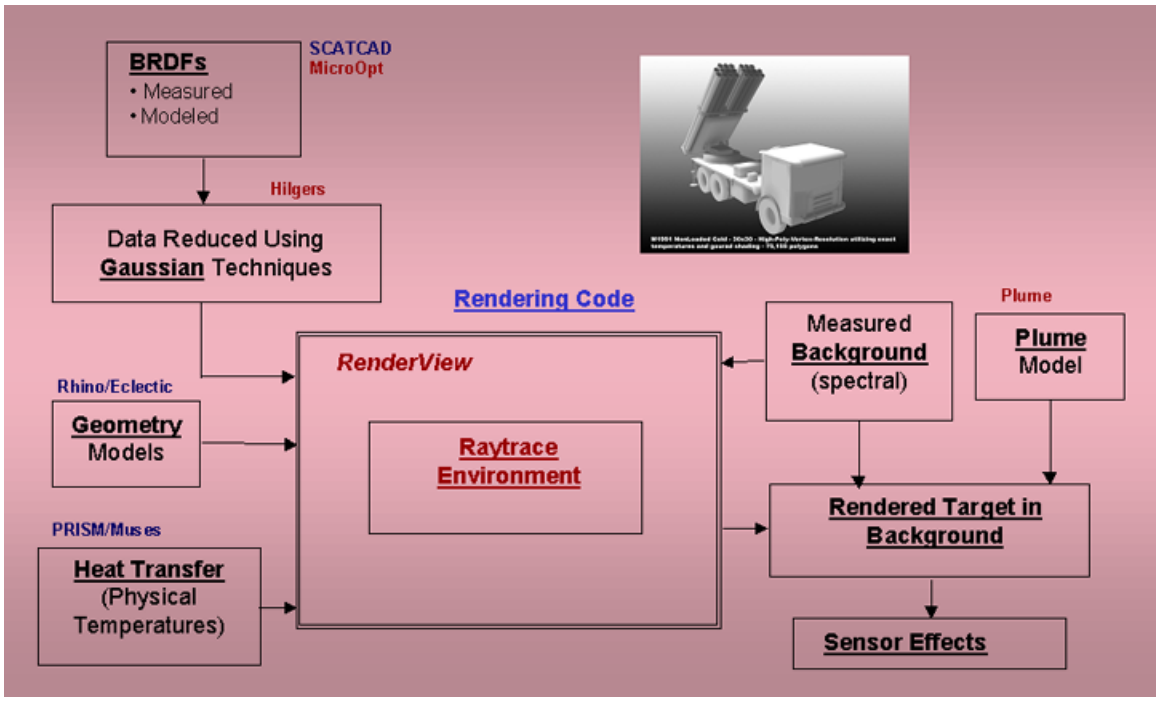

Figure 3: This block diagram shows the critical elements of the *RenderView* modeling process starting with the geometry and reflectance and ending with a photo-realistic image.

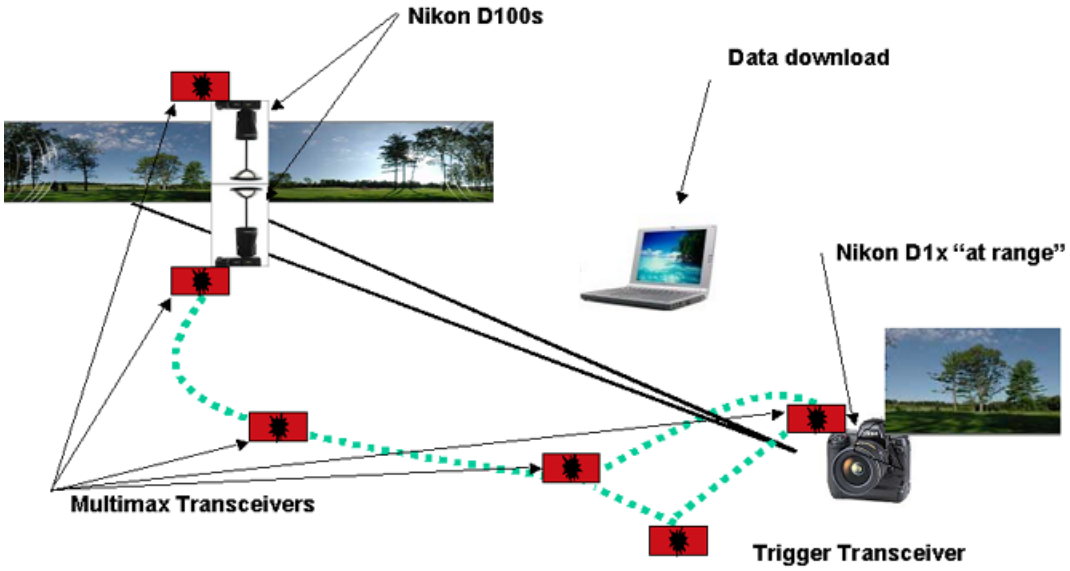

Figure 4: Schematic showing the scene data collection process for *RenderView*.

2.2 Inclusion of Solar Irradiance

Using commercial digital cameras to measure the illumination field for rendering input means that the maximum dynamic range of the image will be 12-bits. A dynamic range of 12-bits is insufficient to fully capture the dynamic range of a scene with direct solar illumination. Consequently, the solar disk and sky near the solar disk is normally saturated. Using MODTRAN4 with the meteorological and geographic data matching the conditions when the data was collected, the intensity of the solar and near solar disk illumination is estimated.

2.3 Rendering Engine

Rendering is the process of collecting all of the energy incident on the polygon and determining the fraction which is reflected toward the sensor. The fraction of each hemispheric component is given by the BRDF. In the thermal domain there is an additional directional emissive component which is also a function of the physical temperature. The reflectance in the direction of the sensor is [5]

$$i'\left(\theta_r,\phi_r\right)=\int_0^{2\pi}\rho''\left(\theta_r,\phi_r,\theta_i,\phi_i\right)i'\left(\theta_i,\phi_i\right)\cos\theta_i\mathrm{d}\omega_i. \tag{1}$$

where ρ'' is the BRDF, i' is the incident intensity, and ω is the solid angle. Solution of (1) yields the intensity of the radiation leaving the surface of the rendered object in the reflected direction, $i'\left(\theta_r,\phi_r\right)$ toward the sensor.

For renderings in the visible band or hyperspectral (1) is evaluated separately for each of the three spectral bands representing red, green and blue (RGB) or for the narrower hyperspectral wavebands. If hyperspectral background data through the visible region is available then the rendering equation is solved for each narrow band. The result is weighted by the observer color response functions and integrated over all wavelengths to obtain the tristimulus values. The tristimulus values are easily transformed to RGB values for display on a monitor.

In building a virtual vehicle, the designer assigns a coating corresponding to a BRDF to every polygon in the geometric model. This is analogous to painting or applying an applique to the actual vehicle. An alternative method, in which sub-polygon resolution is achieved for high resolution camouflage patterning is to use texture maps. The texture map is used as a pointer to the coating properties.

A C++ class library has been developed in which the BRDFs are described as functional objects. These functional objects are tied to a BRDF database (which will also be encapsulated in C++ class objects) which provides the actual reflectance data or function parameters for a given material. The ability to fully describe and assign the correct BRDF to each polygon in the geometric vehicle model opens the door to producing truly photo realistic renderings.

2.4 Shadowing and "At-Range" Atmospheric Effects

In the *RenderView*model, two distinct cases must be considered to account for shadows, facet shadowing and terrain shadowing. Facets which do not have direct line of sight to the solar disk return a lower intensity as a function of the rendering process and are thus shadowed and the shadow intensity is correct. Realistic shading of the surrounding terrain by the inserted vehicle is somewhat more problematic due lack of knowledge of the reflectivity of the background. The background which would be shadowed is part of the "at range" data. Consequently, the effect of vehicle shadowing of the terrain features can not be accounted for in a straightforward manner. An expedient solution is to empirically determine the terrain shadow intensity. A segment of the terrain which is shadowed is identified and the intensity is extracted. These values are inserted in the segments of terrain which are shadowed by the vehicle. Consequently, the vehicle and the shadow area in which the shadow depth is approximated is inserted into the "at range" image.

Atmospheric effects in the line of sight are well understood. Of particular interest in the visible spectrum is how the atmosphere acts to desaturate and shift the color through scattering and attenuation towards the blue end of the spectrum . Psychologists and artists call this phenomena aerial perspective. Psychologists assert that these effects are a fundamental depth cue that humans use to estimate distances, and the only absolute depth

cue available for distant unfamiliar objects. Given the impact on the human perception process, reproducing the at-range blue scattering effects on rendered objects is crucial.

In the absence of measured or modeled atmospheric conditions, an empirical approach has been developed for estimating effect of atmosphere on the vehicle signature in the visible band. Samples are taken of the RGB values of a number of features that can be found both in the foreground and at the range of interest, typically vegetation in the "at range" image. A least-squares fit is performed based on these data pairs and the resulting function is used to adjust the rendered vehicle data to simulate the desired range affects.

To further enhance the realism of the rendering several addition steps are taken including partial occlusion of the target by vegetation, depression of the vehicle into the terrain, simple sensor blurring and the addition of noise. These steps are accomplished using Adobe Photoshop image processing software. There is some question in how to do the blurring step. One approach is to sample the image and the render the vehicle at twice Nyquist sampling for the eye, which is approximately 240 pixels per degree. Place the vehicle in the image and then add a slight Gaussian blur and then delete every other row and column. This reduces the sampling to Nyquist and slightly softens the edges between the vehicle and the background.

2.5 Verification Efforts For *RenderView*

Validation is an ongoing process as enhancements are implemented and more measured data becomes available. Energy conservation in the renderings is fundamental. For example, if energy is not conserved more energy can be received than is incident on the surface resulting in the object becoming too bright in comparison its environment. The opposite can also occur and the resulting render will be too dark.

As a first step in the validation process the results from the rendering of simplistic geometries and BRDF's are compared against the analytic results. The complexity of the geometric models used for the renderings of vehicles preclude comparisons between the results from *RenderView* and analytic results. Furthermore, in most cases in our production renderings the Sanford-Robertson BRDF model [6, 7] is used.

The first test for energy conservation was performed on a cube using a BRDF that was completely diffuse and isotropic. The global illumination field was constant over the entire hemisphere above the cube. The renderer evaluates (1) by approximating the integral by the following summation

$$i'\left(\theta_r,\phi_r\right)=\sum_{j=1}^{n_\theta}\sum_{k=1}^{n_\phi}\rho''\left(\theta_r,\phi_r,\theta_{ik},\phi_{ij}\right)i'\left(\theta_{ik},\phi_{ij}\right)\cos\theta_{ij}\sin\theta_{ij}\Delta\theta_{ik}\Delta\phi_{ij}. \tag{2}$$

A perfectly diffuse reflector (1) can be evaluated analytically by integrating

$$i'\left(\theta_r,\phi_r\right)=\int_0^{2\pi}\frac{R}{\pi}B\cos\theta_i\mathrm{d}\omega_i. \tag{3}$$

Where R is the total hemispherical reflectivity and B is the intensity of the uniform illumination. Performing the integral in (3) results in

$$i'\left(\theta_r,\phi_r\right)=RB. \tag{4}$$

The result given in (4) makes intuitive sense: the light reflected off the surface equals the light incident B times the total reflectivity R. The results from *RenderView* for the isotropic diffuse reflecting surface matched the analytical result to 3 figures.

A more sophisticated test of *RenderView* to check the colormatching is to render a Macbeth Colorchecker. The spectral reflectivity, $rho(\lambda)$, of each of the tiles is well known. In addition, the spectral response of a typical color digital camera is also well known. The average reflectivity, $\overline{\rho}$, for each R, G, and B channel, for each ith tile is given by

$$\overline{\rho}_k=\frac{\int_0^\infty\rho_i(\lambda)\overline{r}_k(\lambda)d\lambda}{\int_0^\infty\overline{r}_k(\lambda)d\lambda}$$

where k represents either the R, G, or B camera channel. Figure 5 shows a rendered Macbeth Colorchecker inserted into an image containing an actual Macbeth Colorchecker. Each color chip was considered to have the properties of a diffuse or constant BRDF. The largest $\delta E_{ab}=10.2$.

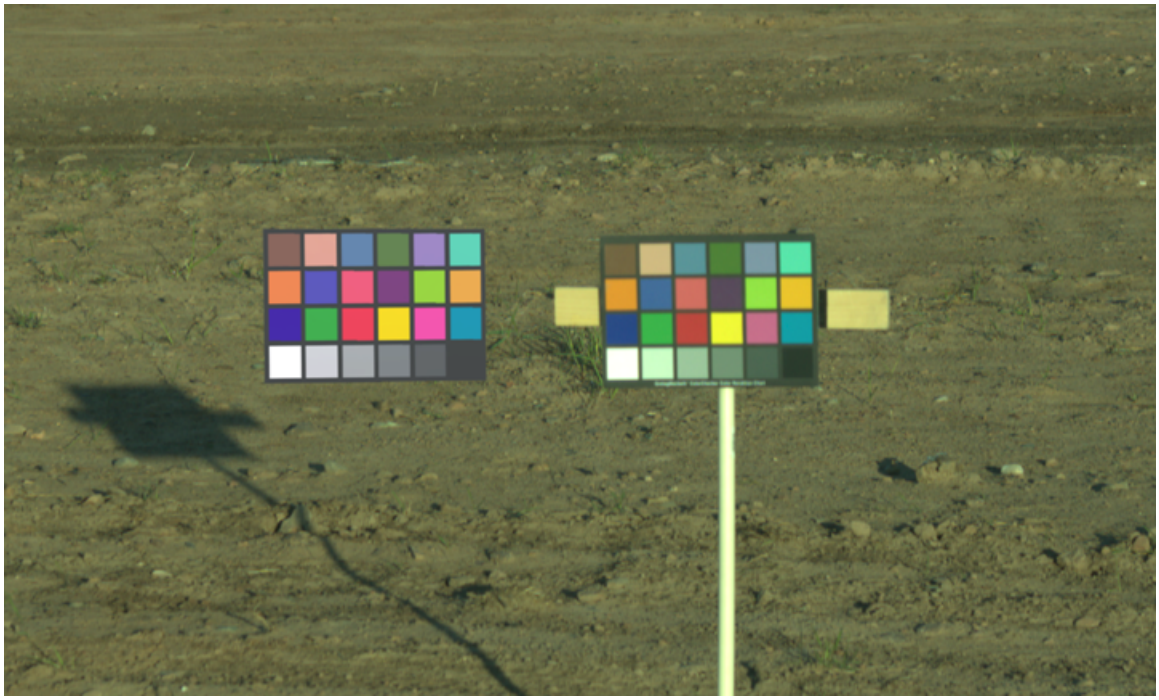

Figure 5: Side by side comparison of a rendered (on the left) and an actual Macbeth Colorchecker.

Table 1: Temperature of three areas on each of the MBTs in figure 6.

	Tool Box	Turret Side	Track Skirt
Physical temp.	28.2	20.6	34.1
MuSES apparent	27.7	20.3	33.2
Rendered diffuse	28.1	20.7	32.4
Std. coating	28.3	20.8	33.0
Specular coating	28.2	20.7	32.7

2.6 Thermal Rendering Example

The visual rendering fidelity is demonstrated in figure 2. The MBT contains a notional camouflage paint scheme made possible through the use of a texture map. A photo-realistic image is the result.

The same MBT was also rendered in the LWIR. In this process the MuSES model was used to calculate the physical temperatures of the exterior surfaces. The meteorology history measure in the site simultaneously with the panoramic and "at range" data acquisition was used for the thermal forcing function. Four vehicles are displayed in figure 6all have the same gray scale. From left to right, the first MBT is just the physical temperatures. The second MBT is the radiosity from MuSES in which the diffuse approximation was used. The third MBT uses a Sandford Robertson BRDF for a standard coating. This coating is fairly diffuse with a broad specular peak. The fourth MBT was again rendered using the Sandford Robertson BRDF with the width of the spectral lobe 3 to 4 times more narrow.

Temperatures were extracted from three locations on each of these vehicles and are presented in Table 2.6. Because the reflectivities are low, the impact of the reflected environment is expected to be minimal and this is shown in Table 2.6. There just isn't a large variation in temperature between the renderings. The reflectivity

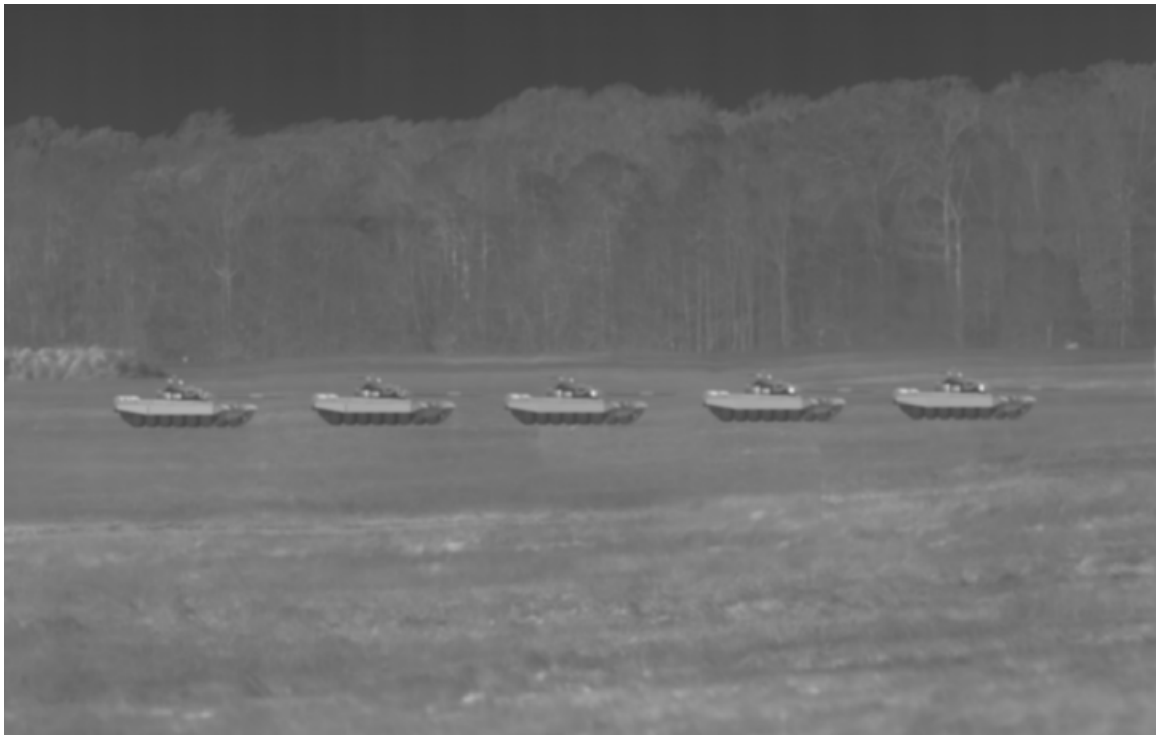

Figure 6: Rendered MBTs, from left to right, first is physical temperatures, second is diffuse approximation in MuSES, third is rendered diffuse, fourth is the Sandford Robertson standard coating, and the fifth is a standard coating with a more narrow specular lobe.

used in the MuSES model is slightly less than what was used in *RenderView*. In general, the small temperature changes appear to move in the right direction. For example, the radiometric temperature for the three vehicle location are lower in MuSES and for the diffuse rendering (with a small exception on the turret) because of the sky contribution. The two vehicles rendered with the Sandford Robertson BRDF models are slightly warmer than the diffuse case because the specular lobe reduces the sky contribution.

3 Conclusions

With *RenderView*, a physics based empirical hybrid model, photo-realistic, first principles, visual and IR modeling is now achievable. In addition, new methods, requirements, and hardware for characterizing backgrounds are currently being developed to support this approach. Also, this approach has the added benefit in that the uncertainty associated with a predictive background model does not factor into the *RenderView* output. New, massive, high resolution predictive background models such as CAMEOSIM and *EOView* are being developed which are photo-realistic and first principles. To support these approaches inexpensive computing clusters will become the norm for future signature modeling and simulation efforts. It is clear that historically, signature modeling technology has been monotonically increasing in complexity and there is no end in sight.

4 Acknowledgments

This work was accomplished in part under funding from the US Army TACOM TARDEC.

References

[1] D. Bornemeier, R. Bennett, and R. Horvath. Target temperature modeling. Technical report, University of Michigan, Willow Run Laboratories, 1969.

[2] J.R. Rapp. A computer model for estimating infrared sensor response to target and background thermal emissions signatures. Technical Report ARBRL-MR-03292, August 1983.

[3] L.K. Balick, R.K. Scoggins, and L.E. Link. Inclusion of a simple vegetation layer in terrain temperature models for thermal infared signature prediction. Technical El-81-4, WES, 1981.

[4] Reynolds. *PRISM Users Manual 3.1.* Keweenaw Research Center, Michigan Technological University, Houghton, Michigan, 3.1 edition, May 1993.

[5] R. Siegel and J.R. Howell. *Thermal Radiation Heat Transfer*. Hemisphere Publishing Corp., 3 edition, 1992.

[6] B.P. Sandford and D.C. Robertson. Infrared reflectance properties of aircraft paint. In *Proc. IRIS Targets, Backgrounds, and Discrimination*, 1985.

[7] J. Jafolla, J. Stokes, D. Thomas, and P. Sarman. A comparison of brdf representations and their effect on signatures. In *Proc. 8th Annual Ground Target Modeling and Validation Conference*, Calumet, MI, August 1997. Signature Research, Inc.